THE HOMOGENIZATION METHOD FOR TOPOLOGY AND SHAPE OPTIMIZATION – SINGLE AND MULTIPLE LOADS CASE

Grégoire ALLAIRE[1] Zakaria BELHACHMI[2] François JOUVE[3]

[1] *Commissariat à l'Energie Atomique, DRN/DMT/SERMA, CEA Saclay, 91191 Gif sur Yvette, France & Laboratoire d'Analyse Numérique, Université Paris 6.*
aler@soleil.serma.cea.fr

[2] *Département de Mathématiques, Université de Metz, Ile du Saulcy, 57045 Metz, France.*
belhach@poncelet.univ-metz.fr

[3] *Centre de Mathématiques Appliquées, URA-CNRS 756, Ecole Polytechnique, 91128 Palaiseau, France.*
francois.jouve@polytechnique.fr

Abstract

This paper is devoted to an elementary introduction to the homogenization method applied to topology and shape optimization of elastic structures under single and multiple external loads. The single load case, in the context of minimum compliance and weight design of elastic structures, has been fully described in its theoretical as well as its numerical aspects in [4]. It is here briefly recalled. In the more realistic context of "multiple loads", *i.e.* when the structure is optimized with respect to more than one set of external forces, most of the obtained theoretical results remain true. However, the parameters that define optimal composite materials cannot be computed explicitly. In this paper, a method to treat numerically the multiple loads case is proposed.

Résumé

Cet article est consacré à une introduction élémentaire à la méthode d'optimisation topologique de formes élastiques – soumises à un ou plusieurs jeux de forces extérieures – par homogénéisation. Le cas mono-chargement, lorsque l'on cherche à minimiser la compliance de la structure élastique sous une contrainte de poids, a été décrit en détails – d'un point de vue théorique et numérique – dans [4]. Il est rappelé brièvement ici. Dans le cas plus réaliste où la structure est optimisée pour résister à plusieurs jeux de forces extérieures (*multi-chargements*) appliqués successivement, la plupart des résultats théoriques restent vrais. Toutefois, les paramètres qui définissent les matériaux composites optimaux ne sont plus calculables explicitement. Nous présentons une méthode pour traiter numériquement le cas multi-chargements.

Keywords: Optimal design, homogenization, shape optimization, topology optimization, sequential laminates.

Mots clé: Optimisation de formes, homogénéisation, optimisation topologique, laminés séquentiels.

1 Introduction

The typical problem of structural optimization is to find the "best" structure which is, at the same time, of minimal weight and of maximum strength. Of course there is some subjectivity in the definition of what is "best". It depends on many different considerations: what is the underlying mechanical model (linear or nonlinear elasticity, plasticity, etc.) ? Are there any constraints on admissible shapes (industrial feasibility, smoothness of the boundary, etc.) ? What kind of stiffness criterion is used (maximum stress, compliance, etc.) ?

Since the focus of this paper is to discuss the homogenization method for structural optimization, some assumptions are required for the definition of a suitable model problem. First of all, we deliberately forget about any feasibility or smoothness constraints on the shape's boundary. Indeed, the process of homogenization (or relaxation) is intimately linked to the possibility of boundary oscillations (small ribs or holes), which are usually prevented by adding the above type of constraints. Then, to complete as far as possible our analysis, we work in the context of linear elasticity, and we choose the compliance (*i.e.* the work done by the load) as a global measure of rigidity.

The main idea of the homogenization method is to replace the difficult "lay-out" problem of material distribution by a much easier "sizing" problem for the density and effective properties of a perforated composite material obtained by cutting small holes in the original homogeneous material. We focus on both the theoretical aspects — the so-called relaxation process — and the numerical aspects of this method.

2 A model problem in shape optimization

We consider a bounded reference domain $\Omega \in \mathbb{R}^N$ ($N = 2, 3$ is the spatial dimension), occupied by a linearly elastic material with isotropic elasticity tensor A (with bulk and shear moduli κ and μ) defined by

$$A = (\kappa - \frac{2\mu}{N}) I_2 \otimes I_2 + 2\mu I_4, \quad 0 < \kappa, \mu < +\infty, \tag{1}$$

The domain Ω is successively submitted to p surface loadings $\{f_i\}_{1 \leq i \leq p}$ on its boundary $\partial\Omega$, and, for each set of forces, equilibrium of the domain is assumed, *i.e.*, $forall Q \;\; N \times N$ symmetric matrix,

$$\int_{\partial\Omega} f_i.n \; ds \; = \; 0, \qquad \int_{\partial\Omega} f_i.Qx.n \; ds \; = \; 0, \qquad \forall i \in \{1, \ldots, p\}.$$

An admissible design ω is a subset of the reference domain Ω obtained by removing one or more holes (the new boundaries created this way are traction-

free). For each f_i, the equations of elasticity for the resulting structure are

$$\left\{\begin{array}{ll} \sigma_i = A\varepsilon(u_i) & \varepsilon(u_i) = \dfrac{1}{2}(\nabla u_i + \nabla^t u_i) \\ \text{div } \sigma_i = 0 & \text{in } \omega \\ \sigma_i \cdot n = f_i & \text{on } \partial\Omega \\ \sigma_i \cdot n = 0 & \text{on } \partial\omega \setminus \partial\Omega. \end{array}\right. \tag{2}$$

The sum of compliances of the design ω is

$$c(\omega) = \sum_{i=1}^{p} \int_{\partial\Omega} f_i \cdot u_i = \sum_{i=1}^{p} \int_{\omega} A\varepsilon(u_i) \cdot \varepsilon(u_i) = \sum_{i=1}^{p} \int_{\omega} A^{-1}\sigma_i \cdot \sigma_i. \tag{3}$$

Introducing a positive Lagrange multiplier λ, the goal is to minimize, over all subsets $\omega \subset \Omega$, the weighted sum $E(\omega)$ of the compliance and the weight (proportional to the volume $|\omega|$), namely to compute

$$\inf_{\omega\subset\Omega} \left(E(\omega) = c(\omega) + \lambda|\omega|\right). \tag{4}$$

The Lagrange multiplier λ has the effect of balancing the two contradictory objectives of rigidity and lightness of the optimal structure (increasing its value decreases the weight). There exists a different formulation of the same structural optimization problem which will be very helpful in the sequel. It is based on the principle of complementary energy which gives the value of the compliance

$$c(\omega) = \sum_{i=1}^{p} \int_{\partial\Omega} f_i \cdot u_i = \sum_{i=1}^{p} \min_{\substack{\text{div } \tau_i = 0 \text{ in } \omega \\ \tau_i \cdot n = f_i \text{ on } \partial\Omega \\ \tau_i \cdot n = 0 \text{ on } \partial\omega \setminus \partial\Omega}} \int_{\omega} A^{-1}\tau_i \cdot \tau_i.$$

Extending the admissible stress τ_i by 0 inside the holes, the compliance is also defined by

$$c(\omega) = \sum_{i=1}^{p} \min_{\substack{\text{div } \tau_i = 0 \text{ in } \Omega \\ \tau_i \cdot n = f_i \text{ on } \partial\Omega}} \int_{\Omega} (\chi_\omega(x)A)^{-1}\tau_i \cdot \tau_i, \tag{5}$$

where χ_ω is the characteristic function of the design ω. The infimum over designs and the minimum over statically admissible stresses can be switched. Then, for a fixed stress, the inside minimization over $\chi_\omega = 0, 1$ is easy. It yields that (4) is equivalent to

$$\inf_{\substack{\tau_i \\ \text{div } \tau_i = 0 \text{ in } \Omega \\ \tau_i \cdot n = f_i \text{ on } \partial\Omega}} \left(F(\{\tau_i\}) = \int_{\Omega} \left\{ \begin{array}{ll} 0 & \text{if all } \tau_i = 0 \\ \displaystyle\sum_{i=1}^{p} A^{-1}\tau_i \cdot \tau_i + \lambda & \text{if at least one } \tau_i \neq 0 \end{array} \right. \right) \tag{6}$$

in the sense that minimizers of (4) and (6) (if any) are related by

$$\chi_\omega(x) = 0 \Leftrightarrow \sigma(x) = 0, \quad \chi_\omega(x) = 1 \Leftrightarrow \sigma(x) \neq 0. \tag{7}$$

As is well known in the mathematical community, in absence of any additional constraints on the admissible designs ω, the objective function $E(\omega)$ may have no minimizer, *i.e.* there is no optimal shape (for striking counter-examples on similar, but simpler, problems, we refer to [30], [31], and to [14] for numerical evidence). This can also be guessed from the other formulation (6) where the objective function $F(\tau)$ is obviously not convex and, as we shall see, not even lower semi-continuous (the correct mathematical notion for proving existence theorems). The physical reason for this non-existence is that it is often advantageous to cut infinitely many small holes (rather than just a few big ones) in a given design in order to decrease $E(\omega)$. Thus, achieving the minimum may require a limiting procedure leading to a "generalized" design consisting of composite materials made by microperforation.

To take into account this physical behavior of nearly optimal shapes, we have to enlarge the space of admissible designs by permitting perforated composites from the start: this process is called *homogenization* (or relaxation). Such a composite structure is determined by two functions: $\theta(x)$, its local volume fraction of material taking values between 0 and 1, and $A(x)$, its effective Hooke's law corresponding to its microstructure. Of course, we need to find an adequate definition of the *homogenized* (or relaxed) objective function $\tilde{E}(\theta, A)$ which generalizes $E(\omega)$. This is done in the next section by using the theories of homogenization and optimal bounds on the effective properties of composite materials. The ultimate goal is twofold: prove an existence theorem for the relaxed formulation of the above structural optimization problem, and find a new numerical algorithm for computing optimal shapes.

For more details on the mathematical theory of relaxation by homogenization in the context of optimal design, we refer to the pioneering works [25], [27], [31]). In the specific framework of computational structural optimization, we refer *e.g.* to [3], [4], [5], [7], [10], [11], [12], [23], [36].

3 Homogenized formulation

In this section we describe the homogenization or relaxation process of the structural optimization problem (4) following [7] and [4]. For simplicity we consider a single loading configuration ($p = 1$) in two or three space dimensions and we omit the i indices introduced in the previous section to identify each loading.

Let $(\omega_\epsilon)_{\epsilon \to 0}$ be a minimizing sequence of nearly optimal shapes for the objective function (4), and denote by χ_{ω_ϵ} their characteristic functions. In the reference domain Ω, we regard it as a fine mixture of the original material A and void (holes). Then, as a result of the homogenization theory, there exists an effective behavior of this fine mixture, *i.e.* a composite material of density

$\theta(x)$, taking any value in the interval $[0,1]$, and a Hooke's law $A^*(x)$ such that

$$\chi_{\omega_\epsilon}(x) \rightharpoonup \theta(x) \text{ weakly in } L^\infty(\Omega),$$

and

$$\chi_{\omega_\epsilon}(x) A \xrightarrow{G} A^*(x)$$

in the sense of H or $G-$convergence. In truth, the homogenization theory works only for composite materials made of two *non-degenerate* phases. Therefore, to be mathematically rigorous the holes are first filled with a weak material, then homogenization takes place, and, in the end, we have to justify the passing to the degenerate limit. For simplicity we skip these details here.

The above homogenization result implies in particular the convergence of the compliance

$$c(\omega_\epsilon) \to \tilde{c}(\theta, A^*) = \int_\Omega A^*(x)^{-1}\sigma \cdot \sigma \tag{8}$$

where the stress σ is now solution of the following homogenized equation

$$\left\{ \begin{array}{ll} \sigma = A^*(x)\varepsilon(u) & \varepsilon(u) = \frac{1}{2}(\nabla u + \nabla^t u) \\ \text{div } \sigma = 0 & \text{in } \Omega \\ \sigma \cdot n = f & \text{on } \partial\Omega. \end{array} \right. \tag{9}$$

For a same value θ of the density, there are many different possible effective Hooke's law A^* corresponding to different microstructures (or geometric patterns of the holes), *i.e.*

$$A^* \in G_\theta$$

where G_θ (the so-called G-closure set at volume fraction θ) is the set of all possible effective Hooke's law with material density θ.

Applying these results, we pass to the limit in the objective function and obtain the homogenized or relaxed functional

$$\lim_{\epsilon \to 0} E(\omega_\epsilon) = \inf_{\omega \subset \Omega} E(\omega) = \min_{\substack{A^* \in G_\theta \\ 0 \le \theta \le 1}} \tilde{E}(\theta, A^*),$$

where

$$\tilde{E}(\theta, A^*) = \tilde{c}(\theta, A^*) + \lambda \int_\Omega \theta(x). \tag{10}$$

This relaxed formulation is not entirely explicit since the precise definition of the G-closure set G_θ is unknown! However, by using again the principle of complementary energy, we can use our knowledge of so-called *optimal bounds* on G_θ that will simplify the relaxed formulation by optimizing the microstructure and eliminating the dependence on A^*. We rewrite the compliance as

$$\tilde{c}(\theta, A^*) = \min_{\substack{\text{div } \tau = 0 \text{ in } \Omega \\ \tau \cdot n = f \text{ on } \partial\Omega}} \int_\Omega A^*(x)^{-1}\tau \cdot \tau. \tag{11}$$

Then, switching the two minimizations and optimizing pointwise the microstructure and density, the relaxed formulation becomes

$$\min_{\substack{\text{div } \tau=0 \text{ in } \Omega \\ \tau\cdot n=f \text{ on } \partial\Omega}} \left\{ QF(\tau) = \int_\Omega \min_{\substack{A\in G_\theta \\ 0\le\theta\le 1}} \left(A^{*-1}\tau\cdot\tau + \lambda\theta \right) \right\}. \tag{12}$$

For a fixed stress τ, the minimization of $A^{*-1}\tau\cdot\tau$ on G_θ is a classical problem in the theory of optimal bounds on effective properties of composite materials see [8] [29]. It has been solved in 2-D in [6], and in 3-D in [2]. In two dimensions, the result is

$$\min_{A^*\in G_\theta} A^{*-1}\tau\cdot\tau = A^{-1}\tau\cdot\tau + \frac{(\kappa+\mu)(1-\theta)}{4\kappa\mu\theta}\left(|\tau_1|+|\tau_2|\right)^2 \tag{13}$$

where τ_1 and τ_2 are the eigenvalues of the 2 by 2 symmetric matrix τ. Furthermore, optimality in (13) is achieved for a so-called rank-2 sequential laminate aligned with the eigendirections of τ.

In three dimensions, the result is messier, and we give it in the special case of Poisson's ratio equal to zero, *i.e.* $3\kappa = 2\mu$ (the general case is not much different in essence, see [2])

$$\min_{A^*\in G_\theta} A^{*-1}\tau\cdot\tau = A^{-1}\tau\cdot\tau + \begin{cases} \dfrac{(1-\theta)}{4\mu\theta}\left(|\tau_1|+|\tau_2|+|\tau_3|\right)^2, & |\tau_3|\le|\tau_1|+|\tau_2| \\ \dfrac{(1-\theta)}{2\mu\theta}\left(\left(|\tau_1|+|\tau_2|\right)^2+|\tau_3|^2\right), & |\tau_3|\ge|\tau_1|+|\tau_2| \end{cases} \tag{14}$$

where the eigenvalues of τ are labeled in such a way that

$$|\tau_1|\le|\tau_2|\le|\tau_3|.$$

Furthermore, optimality in the first regime of (14) is achieved by a rank-3 sequential laminate aligned with the eigendirections of τ, while in the second regime it is achieved by a rank-2 sequential laminate aligned with the two first eigendirections of τ.

After this crucial step, the minimization over θ can easily be done by hand, which completes the explicit calculation of the relaxed formulation. Remark also that, by virtue of formulae (13) and (14), the pointwise optimization of the density yields $\theta = 0$ if and only if $\tau = 0$, which means that holes are created only where the stress vanish.

The final result is the following

Theorem 3.1 *Problem (10), or equivalently (12), is the homogenized or relaxed formulation of the original problem (4), or (6), in the sense that there*

exists at least one "generalized" or homogenized optimal design (θ, A^*)*, which is the limit of a minimizing sequence of "classical" shapes* ω_ϵ*, and the minimal values of the original or homogenized energies coincide*

$$\inf_{\omega \subset \Omega} E(\omega) = \min_{\substack{A^* \in G_\theta \\ 0 \leq \theta \leq 1}} \tilde{E}(\theta, A^*).$$

Its proof can be found in [7] for the 2-D case, and in [4] for the 3-D case. Remark that the homogenization process does not change the physics of the problem. Indeed, an homogenized optimal design is just a limit of nearly optimal classical designs, and the homogenized energy is precisely the average of the original energy when the nearly optimal classical designs oscillate (*i.e.*, have many holes or ribs). In particular, any possible solution of the original problem is also a solution of the homogenized problem.

3.1 Non-uniqueness

There is a wild non-uniqueness for the optimal homogenized designs. In the first place, the optimal microstructure is not always unique. For example, the optimal sequential laminate is not uniquely defined in the case of an hydrostatic stress τ proportional to the identity I_2 (any orthonormal basis of $\mathbb{R}^N$ is a set of eigenvectors of τ and thus a set of lamination directions). It can be checked that different directions lead to different homogenized Hooke's law. But there is another type of non-uniqueness of the microstructure: sequential laminates are not the only known class of optimal microstructures (although probably the easiest to work with). The so-called concentric spheres construction [21] (generalized in [37] to confocal ellipsoids), or the periodic arrangement of adequately shaped inclusions in [38] (see also [19]) are also optimal in specific situations.

Another possible non-uniqueness is that of the homogenized density. For example, in the case of a constant hydrostatic boundary condition $f = pI_2$, the homogenized stress is exactly equal to pI_2 and the average compliance is $\frac{Np^2}{\kappa^*}$ where κ^* is the so-called Hashin-Shtrikman upper bound on the bulk modulus [22]. A generalized optimal design is given as a composite material of constant density θ determined by the values of p and λ. But there are also an infinite number of classical optimal shapes obtained by the well-known concentric spheres constructions (see *e.g.* [15]). It amounts to cover the domain Ω by a dense packing of non-overlapping spheres of all sizes. Then, in each sphere, a concentric spherical hole is cut, and its radius is determined in a manner such that the volume fraction of material is precisely θ. This yields a perforated domain Ω with infinitely many disjoint spherical holes of all sizes. It is a classical result that, for such a perforated domain ω under the hydrostatic boundary condition $f = pI_2$, the exact compliance is equal to the homogenized compliance. Therefore, $E(\omega)$ being equal to the minimal relaxed energy, ω is also

an optimal shape. Remark that this type of classical optimal shapes would be very difficult to compute numerically, partly because they are not homogenized or averaged. Indeed its boundary is very complex since it involves an infinite number of connected components on various length scales. Therefore, even in this case, the relaxed problem is more practical from a numerical standpoint.

3.2 Link to Michell trusses

An important feature of the optimal sequential laminates is that they are "smart" materials. The optimal microstructure (namely the rank-N laminate) adapts itself to the stress that it should sustain, by aligning its lamination directions with the principal directions of the stress and adopting in each layer a volume fraction which is controlled by the values of the principal stresses. This correlation between microstructure and stress is a rigorous consequence of the homogenization theory and not a postulate. In particular in 2-D we recover the well-known principle of material economy in frame-structures due to Michell [28].

In two dimensions, when the Lagrange multiplier λ goes to infinity, it is easily seen (see [7]) that the relaxed problem is asymptotically equivalent to the so-called *Michell trusses* problem

$$\min_{\substack{\text{div } \tau=0 \text{ in } \Omega \\ \tau\cdot n=f \text{ on } \partial\Omega}} \int_\Omega (|\tau_1| + |\tau_2|)\, dx,$$

where τ_1, τ_2 are the eigenvalues of the stress τ. There is a rich literature on this problem (see *e.g.* [1], [24], [34], [35]). Note that this limiting case of the relaxed formulation may explain the success of our computations, and more precisely the fact that many of our optimal structures look like a network of trusses, or bars, in 2-D.

3.3 Multiple loads case

So far, we concentrated only on the so-called "single load" problem. Most of the obtained theoretical results hold true for the multiple loads problem stated in Section 2. The homogenized problem is

$$\min_{\substack{A^*\in G_\theta \\ 0\le\theta\le 1}} \left\{ \tilde{E}(\theta, A^*) = \sum_{i=1}^{p} \int_\Omega A^*(x)^{-1}\sigma_i \cdot \sigma_i + \lambda \int_\Omega \theta(x) dx \right\}$$

However, the optimization over the microstructure A^* cannot be done analytically. In other words an explicit formula for the optimal microstructure is not available. We simply know that optimality is attained in the class of sequential

laminates, but the direction of laminations and the proportions are not specified. For any number p of loading configurations, the number of laminations is never larger than 3 in 2-D [9], and 6 in 3-D [18]. Therefore, the optimal microstructure has to be determined numerically rather than through an explicit formula. Numerical methods to compute these optimal composites will be discussed in Section 5.

4 Computational aspects

Up to now, using homogenization theory and introducing a relaxed formulation might appear to be just a trick for proving existence theorems. In fact its importance goes much further, and it is at the root of new numerical algorithms for computing optimal shapes. Indeed, it permits to separate the minimization process in two different tasks: first, optimize locally the microstructure (that is the effective Hooke's law A^*) with explicit formula, second, minimize globally on the density $\theta(x)$. This has the effect of transforming a difficult "free-boundary" or layout problem into a much easier "sizing" optimization problem in a fixed domain. It has many advantages: on the one hand, the cost of a computation is very low compared to traditional algorithms since the mesh is the same for any shape in the iterative process of optimization; on the other hand, it behaves as a topology optimizer and the final optimal shape may have a topology completely different from that of the initial guess. As such the homogenization method is usually applied as a pre-processor for classical shape optimization algorithms (see, *e.g.*, [33]): first, an optimal topology is found by homogenization, then the resulting shape is optimized by a sensitivity analysis of its boundary (for numerical examples, see [32]). Note that classical shape optimization algorithms work with a fixed topology, namely that of the initial guess, and are therefore unable to optimize it (with the noticeable exception of the so-called bubble method [16]).

The key features of homogenization-based algorithms have been first recognized by M. Bendsoe and N. Kikuchi in their pioneering work [12]. Many generalizations have appeared since then. Here, we shall follow our approach advocated in [7], [5], [4].

4.1 A numerical algorithm for 2 and 3-dimensional shape optimization

The proposed numerical algorithm for shape optimization, is based on the homogenization method as described in the previous section. The key idea is to compute "generalized" optimal shapes for the relaxed formulation, rather than "classical" shapes which are merely approximately optimal for the original

formulation. Recall that the relaxed or homogenized objective function is

$$\min_{\substack{\text{div } \tau_i=0 \text{ in } \Omega \\ \tau_i \cdot n = f_i \text{ on } \partial\Omega}} \left\{ QF(\{\tau_i\}) = \int_\Omega \min_{\substack{A \in G_\theta \\ 0 \le \theta \le 1}} \left(\sum_{i=1}^{p} A^{*-1} \tau_i \cdot \tau_i + \lambda \theta \right) \right\}. \tag{15}$$

We introduced a so-called "alternate directions method", that is based on two key ideas. The first one is to consider the above relaxed problem as a minimization problem not only for the stress, but also for the structural parameters, the density θ, and the microstructure A^*. The second key idea is not to try to minimize directly in the triplet of variables $(\{\tau_i\}, \theta, A^*)$, but rather to adopt an iterative approach and minimize separately and successively in the design variables (θ, A^*) and in the field variable $\{\tau_i\}$. The minimization in τ_i for fixed design variables amounts to the resolution of p linear elasticity problems for the structure defined by the previous design variables. In the single load case ($p = 1$), the minimization in (θ, A^*) for a fixed stress field is explicit in view of the formulae (13) and (14). If $p > 1$ (multiple loads case), the minimization in A^* for p fixed stress fields cannot be done explicitly. It is performed numerically, in each cell of the mesh, as described in the next section. The optimization in θ remains explicit. In both cases, the algorithm is structured as follows:

1. Initialization of the design parameters (θ_0, A_0^*) (for example, taking $\theta_0 = 1$ and $A_0^* = A$ everywhere in the domain).
2. Iteration until convergence:
   (a) Computation of $\{\tau_i^n\}_{1 \le i \le p}$ through p linear elasticity problems with $(\theta_{n-1}, A_{n-1}^*)$ as design variables.
   (b) Updating of the design variables (θ_n, A_n^*) by using the stresses τ_i^n in the explicit optimality formulae (single load case $p = 1$) or in numerical procedure (multiple loads case $p > 1$).

The alternate direction algorithm is apparented to two previously known methods: that of [12], [36], and that of [7]. It is a version of the well-known optimality criteria algorithm (see *e.g.* [35]).

Convergence is always achieved since the above iterative process always decreases the value of the objective function at each iteration. In practice, convergence of this iterative algorithm is detected when the objective function becomes stationary, or when the change in the design variables becomes smaller than some preset threshold.

Our experience shows that this algorithm works very well and converges smoothly in a relatively small number of iterations (between 10 and 100, depending on the desired accuracy). Furthermore, it seems to be insensitive to

the choice of initial guess and convergent under mesh refinement, suggesting uniqueness of a global minimum (at least numerically). However, as expected, it usually produces "generalized" optimal designs that include large regions of composite materials with intermediate density. Figure 2 shows the resulting optimal density of material for the "2-D bridge" problem defined by the loading configuration and the boundary conditions shown on Figure 1. White regions are void, black regions are filled with material A, and grey regions represent composite material – fine mixture of A and void. Figure 6 shows, as an example of 3-D numerical result, an optimal 3-D bridge for the load and boundary conditions set on Figure 5.

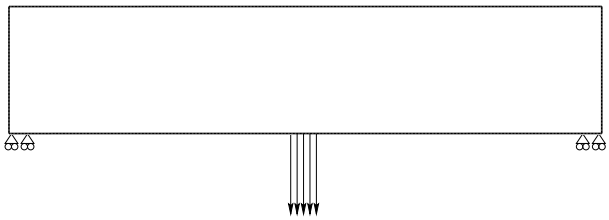

Figure 1: *Loading configuration and boundary conditions for the 2-D bridge.*

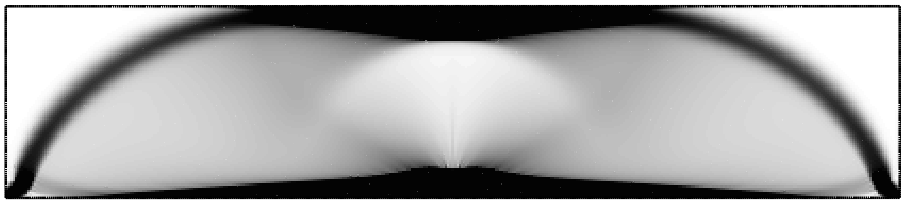

Figure 2: *Generalized solution for the 2-D bridge.*

4.2 Some technical issues

The generalized Hooke's laws computed at each iteration turns out to be singular, an undesired feature when solving linear elasticity problems. This singular behavior has several sources.

First, we note that the effective tensor is equal to zero when the density vanishes. Implicitly, the corresponding stress field should vanish simultaneously. This problem, which occurs in 2 and 3-D, is easily circumvented by imposing a positive threshold on the density. In practice, the smallest admissible value of θ is fixed around 10^{-3}. Numerical experiments suggest that the choice of such a value is not important.

We also remark that rank-1 and rank-2 laminates produce degenerate Hooke's

laws. In 3-D, the lamination proportions in each (orthogonal) direction are forced to be greater than zero. Consequently, the algorithm only uses rank-3 laminates, which are non-singular. In 2-D, rank-1 laminates are eliminated like in the 3-D case. However, the algorithm uses rank-2 laminates as optimal microstructures. The singularity is avoided by adding a small correction term to the composite Hooke's law.

When using $P1$ or $Q1$ finite elements in a displacement formulation, our algorithm is subject to checkerboard instabilities for the density θ similar to those reported in [11], [23]. Such a phenomenon does not occur if a stress-based or complementary formulation is used. Also, these instabilities do not appear if the displacements are computed using higher order elements ($Q2$ for example), while the lamination parameters are computed with only piecewise constant stresses.

The numerical onset of checkerboard patterns is still mysterious. In practice, such instabilities only appear after a large number of iterations, when the convergence criterion is very tight.

In 2-D calculations, we eliminate these instabilities with a method used to filter pressure fields in a Stokes flow computation [13]. Once the piecewise constant optimal densities θ_i^n are determined, we project them on super-elements, which are clusters of 4 adjacent elements, so as to eliminate the checkerboard mode and preserve the overall density. We have not experienced any checkerboard patterns in 3-D calculations.

4.3 Penalization of intermediate densities

As already explained the numerical computations deliver relaxed, or generalized, optimal shapes – a density of material – rather than classical optimal shapes for the original formulation – a characteristic function of the material domain. In other words, our method produces a layout of material, which, as expected, includes large region of composite materials with intermediate density. From a practical standpoint, this is an undesirable feature since the primary goal is to find a real shape – a density taking only the values 0 or 1! This drawback is avoided through a post-processing technique that *penalizes* composite regions. The goal is to deduce, from the optimal densities, a quasi-optimal shape. In loose terms, the solution of the relaxed problem is projected onto the set of classical solutions of the original problem, in the hope that the value of the objective functional will not increase too much in the process.

The strategy is as follows. Upon convergence to an optimal density, we run a few more iterations of our algorithm where we *force* the density to take values close to 0 or 1. This changes the optimal density and produces a quasi-optimal shape. In practice, instead of updating the density with the true optimal density θ_{opt}, a value $\theta_{pen} = (1 - \cos(\pi\theta_{opt}))/2$ is used. Numerical experiments

show few variations in penalized designs for different choices of θ_{pen}.

Of course, the procedure is purely numerical and mesh dependent. The finer the mesh, the more detailed the resulting structure will appear at the outset of the penalization process. The method works well, because the relaxed design is characterized not only by a density θ but also by a microstructure A^*, which is hidden at the sub-mesh level. The penalization tends to reproduce the microstructure at the mesh level.

Figure 3 shows the resulting penalized design for the 2-D bridge. Convergence history of the cost-function has been plotted on Figure 4. Note the small relative difference in performance between the converged composite design (iteration 73) and the penalized design, compared to the performance of the initial configuration (iteration 1) where the whole domain is filled with A material.

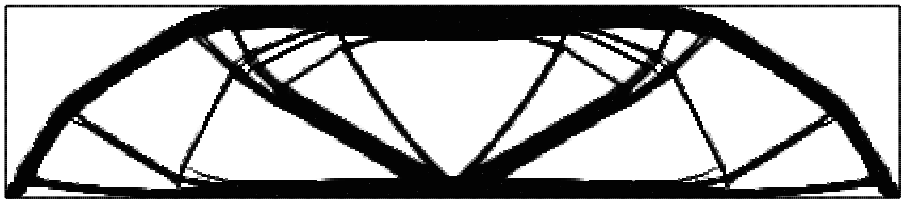

Figure 3: *2-D bridge: penalized design.*

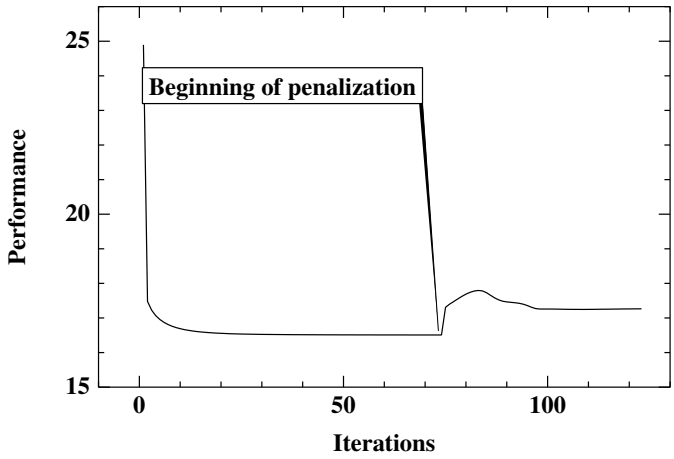

Figure 4: *2-D bridge: convergence history.*

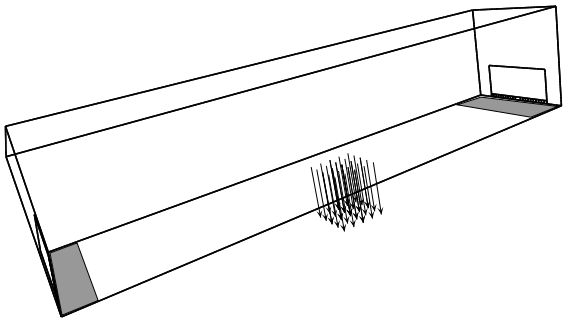

Figure 5: *Computation domain, loading configuration and boundary conditions for a 3-D bridge. The domain is held fixed on grey regions.*

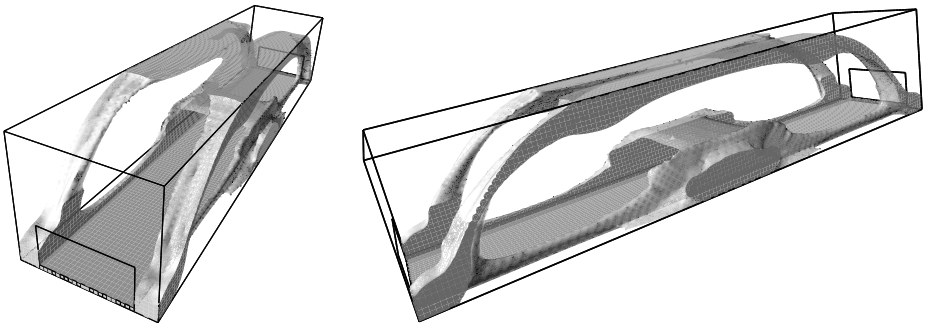

Figure 6: *Optimal 3-D bridge from two different points of vue. The domain of* $\{\theta \geq 0.3\}$ *for the composite solution is represented.*

4.4 Homogenization versus "fictitious material"

The preceding numerical algorithm for computing optimal shapes may seem a little bizarre: we spent a long time to introduce homogenization theory, a proper optimal microstructure, and complicated formulas for updating the design variables, and in the end, one could think that we are simply throwing away everything since we penalize and get rid of all the composite materials! Some authors (see *e.g.* [35]) have thus been led to propose a simpler approach that is sometimes called "fictitious material" method and coincides with the use of the *convexification* of the original problem. Their argument is the following: the idea of working with a density instead of a real shape is a good one, but, since in the end all intermediate densities are eliminated by penalization of the final result, why not suppress the delicate concept of a real microstructure and rather work simply with the same material A with a varying density (or thickness in the language of plate theory) ? Of course, such an approach has the real advantage of being straightforward to implement. However, as we shall

see, its results are not as good as the ones of the homogenization method.

The "fictitious material" approach amounts to consider the following state equation

$$\left\{ \begin{array}{ll} \sigma = \theta(x) A\varepsilon(u) & \varepsilon(u) = \frac{1}{2}(\nabla u + \nabla^t u) \\ \text{div } \sigma = 0 & \text{in } \Omega \\ \sigma \cdot n = f & \text{on } \partial\Omega \end{array} \right. \tag{16}$$

where $\theta(x)$ is a density function taking its values between 0 and 1. The goal is still to minimize, over all possible density, the weighted sum of the compliance and the weight, namely to compute

$$\min_{0 \le \theta(x) \le 1} \left(c(\theta) + \lambda \int_\Omega \theta(x) \right), \tag{17}$$

where the compliance is defined by

$$c(\theta) = \int_{\partial\Omega} f \cdot u = \int_\Omega (\theta(x) A)^{-1} \sigma \cdot \sigma. \tag{18}$$

By using the principle of complementary energy and switching the two minimizations, it is easily seen to have the following equivalent formulation which is the convexification of the stress-based formulation.

$$\inf_{\substack{\text{div } \tau = 0 \text{ in } \Omega \\ \tau \cdot n = f \text{ on } \partial\Omega}} \left(CF(\tau) = \int_\Omega \left\{ \begin{array}{ll} A^{-1}\tau \cdot \tau + \lambda & \text{if } A^{-1}\tau \cdot \tau \ge \lambda \\ 2\sqrt{\lambda A^{-1}\tau \cdot \tau} & \text{if } A^{-1}\tau \cdot \tau \le \lambda \end{array} \right. \right) \tag{19}$$

Since it is a convex minimization problem, existence of optimal solutions is straightforward. By definition, the different energies of the stress τ satisfies $F(\tau) \ge QF(\tau) \ge CF(\tau)$, where the inequalities are strict for most choices of τ.

We have implemented numerically this convex formulation by using the same "alternate directions" strategy as before: for a given density θ, we compute the stress σ solution of the linear elasticity state equation, then we update the design variable θ by the following optimality relationship

$$\theta(x) = \left\{ \begin{array}{ll} 1 & \text{if } A^{-1}\sigma \cdot \sigma \ge \lambda \\ \sqrt{\lambda^{-1} A^{-1}\sigma \cdot \sigma} & \text{if } A^{-1}\sigma \cdot \sigma \le \lambda \end{array} \right. \tag{20}$$

This algorithm converges quickly and smoothly, and we supplement it with the same penalization procedure as before. In general, the fictitious penalized design fails to have the same degree of complexity and detailed patterns as the homogenized penalized design (its energy $E(\omega)$ is indeed larger).

This sensibly worse behavior of the fictitious material approach takes its roots in the fact that there are no implicit microstructure hidden at the submesh level like for the homogenization method. Thus, penalization does not reveal any structure which was waiting to appear at the grid level. In other words, a solution of the convex formulation lies far away from any quasi-minimizer of the original formulation.

5 Multiple loads case

The major difference between the single load case and the multiple load one, is that there are no explicit algebraic formulae to compute the lamination variables (both directions and proportions) in the last case. Although we know from theoretical results (cf. previous section) that rank-3 sequential laminate in two-dimensional case, and rank-6 in three-dimensional case, are the optimal laminates, we are not able to compute them explicitly. Therefore, we have to perform numerically this computation using some minimization algorithm. This optimization will occur at each iteration of our alternate directions algorithms, in each cell of the mesh.

A different approach of multiple loads optimization has been advocated in [26], [20]. It is based on the fact that sequential laminates are represented by a positive measure on the unit sphere (giving the proportions of material in each direction of lamination) whose only relevant informations for optimization purposes are its fourth-order moments. The idea is thus to optimize in terms of these fourth-order moments rather than in terms of the original measure on the unit sphere. This approach is certainly more efficient than ours but is unfortunately restricted to the two-dimensional case since the set of fourth-order moments is explictly known only in this case (see [9]).

5.1 Sequential laminates and lamination formulae

Given p fixed stress tensors $\{\tau_i\}_{1\leq i\leq p}$, we want to find

$$F(\tau,\theta) = \min_{A^*\in G_\theta} \sum_{i=1}^{p} A^{*-1}\tau_i\cdot\tau_i, \tag{21}$$

We know that optimality is achieved for a particular class of material named *sequential laminates* (see [8]). These materials are fully described with a few numbers of parameter: the number of laminations (*rank* of the laminate), the lamination directions and the proportions of lamination in each direction. Furthermore, given these parameters, the effective Hooke's law can be computed explicitly. For example, if A is the elasticity tensor of the initial material – assumed to be isotropic for simplicity – with $\lambda \geq 0$ and $\mu > 0$ its Lamé coefficients, the effective Hooke's law of a rank-n laminate of A with void in proportion θ and $(1-\theta)$ can be written (see [17])

$$A^{*-1} = A^{-1} + \frac{1-\theta}{\theta}\left(\sum_{i=1}^{n} m_i f_A^c(e_i)\right)^{-1}, \tag{22}$$

where $\{m_i\}_{1\leq i\leq n}$ are the lamination proportions ($0\leq m_i\leq 1$, $\sum_{i=1}^n m_i = 1$), $\{e_i\}$ are the directions of lamination ($|e_i| = 1$) and $f_A^c(e_i)$ are fourth order

tensors defined, for any $N \times N$ symmetric matrix ξ by

$$f_A^c(e_i)\xi \cdot \xi = A\xi \cdot \xi - \frac{1}{\mu}|A\xi e_i|^2 + \frac{\mu+\lambda}{\mu(2\mu+\lambda)}((A\xi)e_i \cdot e_i)^2.$$

Equation (21) can therefore be rewritten as

$$F(\tau, \theta) = \min_{A^* \in L_\theta} \sum_{i=1}^{p} A^{*-1}\tau_i \cdot \tau_i, \tag{23}$$

where L_θ is the set of all tensors A^* defined by formula (22).

Considering the function to minimize, we expect that the minimization over the lamination directions gives rise to some numerical difficulties; indeed, the lack of convexity with respect to $\{e_i\}$ variables may lead to unstable and expensive numerical computations.

To avoid this drawback, the idea is to keep fixed a given number n of directions – sufficiently large to allow a good accuracy – and to minimize only on lamination proportions since formula (22) is convex in $\{m_i\}$. Hence, in 2-D, we discretize the space uniformly by setting

$$e_k = \left(\cos\frac{k\pi}{n}, \sin\frac{k\pi}{n}\right), \qquad 0 \le k \le n-1$$

and in 3-D, in a less uniform way when n is chosen such that $n = n_s^2$

$$e_k = \left(\cos\frac{l\pi}{n_s}\cos\frac{m\pi}{n_s}, \sin\frac{l\pi}{n_s}\cos\frac{m\pi}{n_s}, \sin\frac{m\pi}{n_s}\right), \quad 0 \le l, m \le n_s - 1.$$

The resulting approximate optimization problem amounts to find

$$\tilde{F}(\tau, \theta) = \min_{\substack{m_k \in [0,1] \\ \sum_{k=1}^{n} m_k = 1}} \sum_{i=1}^{p} \left\{ A^{-1}\tau_i \cdot \tau_i + \frac{1-\theta}{\theta}\left(\sum_{k=1}^{n} m_k f_A^c(e_k)\right)^{-1} \tau_i \cdot \tau_i \right\}. \tag{24}$$

The minimization in θ can be handled separately (and explicitly as function of fixed $\{m_k\}$). Hence we have to solve a convex optimization problem in $\{m_k\}$ with both equality and inequalities constraints.

5.2 Minimization over lamination proportions

The minimization problem over proportions can be handled by different classical algorithms; in our context the choice of an algorithm needs to satisfy some criteria. Since the minimization process is performed locally for each cell of the mesh, and for each iteration of the alternate directions method, the algorithm

chosen must combine a good rate of convergence with minimal cost in terms of computation time.

The difficult point of this optimization consists in a good treatment of the constraints. Newton-like methods – like the interior points method – involving inversions of the Hessian matrix have been excluded for their CPU cost: computation of the Hessian (n^2 coefficients) and a $n \times n$ matrix inversion at each iteration.

After numerous tries with different gradient-type algorithms, our choice has been fixed on the following: the equality constraint $\sum_{k=1}^{n} m_k = 1$ has been eliminated taking for example $m_1 = 1 - \sum_{k=2}^{n} m_k$. Numerical test have shown that the choice of the eliminated variable does not bias the solution. After this transformation, the problem becomes an optimization problem with only inequalities constraints. It is treated by a classical projected gradient algorithm. Its efficiency depends strongly on the good performance of the line-search algorithm used along the descent directions.

5.3 Orthogonal directions method

This method is a fast alternative to the previous one. It is less accurate than the multiple loads method exposed above, but faster and sometimes, at least when one of the loads is preeminent, gives good results.

The method is based on the following key idea: use rank-N laminates in N dimensions (as it has been rigorously established in the single load case), and align the lamination directions on the principal directions of the stronger stress tensor in each mesh cell. Hence, the minimization problem reduces to a minimization over one variable (the proportion m_1 since $m_1 + m_2 = 1$) in 2-D and two variables in 3-D. When the lamination directions are fixed, the optimization in m_1 can be done explicitly in 2-D, and is easy to perform numerically in 3-D.

6 Numerical results

The algorithm has been first tested independently from the shape optimization program: for some fixed stress tensors $\{\tau_i\}$ we tried to solve, as fast as possible, and with the best accuracy problem (24). Figure 7 shows the values of $\tilde{F}(\tau, \theta)$ obtained as function of the number of directions. The energy is globally decreasing with the rank of the laminate chosen. Note that the energy does not monotonically decrease with the number of directions: for particular values of n it may happen that the "good" directions corresponding to the rank-3 laminate (in 2-D) that reaches the energy bound fall in the set of fixed directions, while some greater values of n can only approximate these directions.

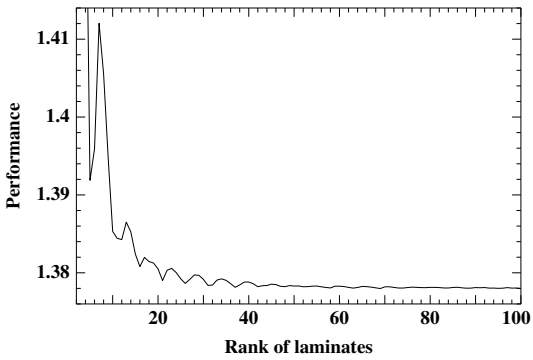

Figure 7:

At this stage, we conclude that the method is robust but quite expensive in CPU-time: the algorithm's cost grows roughly linearly with n. But in the context of the shape optimization algorithm we must do an important remark. As showed by Figure 4, the global design converges rapidly in the very first iterations of the method. Only small changes – but essential to the good convergence of the penalization process – occur after this first stage. The gradient method, when initialized with a good initial guess, can improve dramaticaly its performance. In our case, we experimented a good acceleration of the gradient algorithm after few iterations, when the global topology is established.

To illustrate the efficiency of the method on a real – industrial – case, we performed the optimization on a benchmark proposed by Peugeot: a suspension triangle. Figure 8 shows the domain to optimize with the boundary conditions and the two loads. Each load corresponds to different situations of driving. The real piece must support successively these two kinds of external forces. The intensity of the second (horizontal) load have been increased in order to balance the respective importance of the two cases.

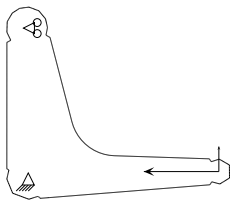

Figure 8: *Boundary conditions and loads for the suspension triangle.*

When optimized separately for each load, the piece is as shown on Figures 10 and 11. The multiple loads optimization gives the shape drawn on Figure 12, more realistic from an automobile engineer point of view.

On Figure 9, the evolution of the objective function is plotted for 4 different methods: rank-n laminates with fixed directions (two cases: $n = 10$ and $n = 25$), convexification (or "fictitious material approach"), and "orthogonal directions" method. As expected, the convexified formulation shows a better performance in the composite phase but becomes less efficient than the other methods after penalization. The penalized design is slightly better with rank-25 than with rank-10 laminates. The "orthogonal directions", far cheaper in CPU time than the rigorous approach using rank-n laminates, gives – for this particular test – acceptable results (comparable to rank-10 laminates). But its convergence, especially when the number of loads becomes large, is not guaranted.

Conclusion

We have presented an efficient method to treat numerically the multiple loads case. This approach leads to better numerical results than those of the "fictitious material" method or of the "othogonal directions" method. Its drawback, at least in the 2-D case, is its cost in terms of CPU time, compared to the approach of [20] or [26]. However, in 3-D it is the only available method. Remark also that in 3-D the relative cost of the lamination proportions optimization is much smaller compared to the solution of the elasticity problem at each iteration. Although the gradient algorithm for computing the lamination proportions can certainly be enhanced by a suitable refinement procedure, our method is already reliable for industrial applications.

Acknowledgments

The second author was supported by a post-doctoral grant from PSA (Peugeot-Citroën) group. We want to thank P. Esmingeaud (from PSA) for his support and for the definition of the test showed on Figures 8 to 12.

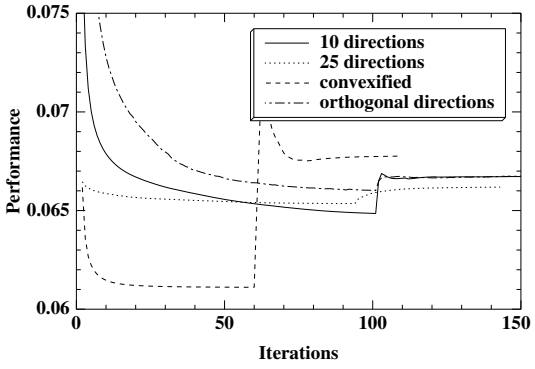

Figure 9:

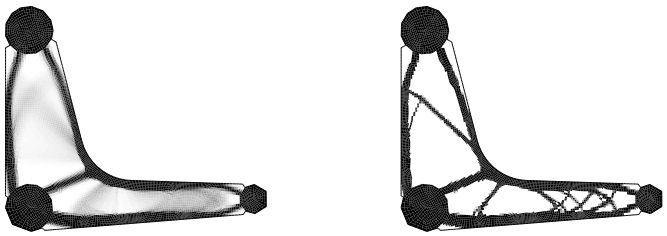

Figure 10: *Composite (left) and penalized (right) solutions of the suspension triangle for the first loading case*

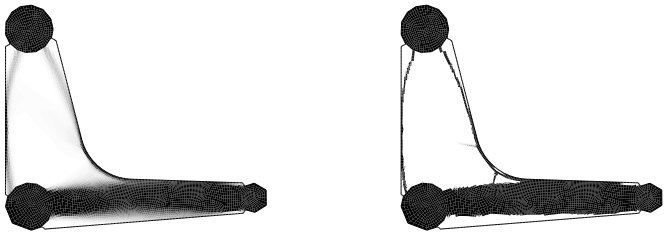

Figure 11: *Composite (left) and penalized (right) solutions of the suspension triangle for the second loading case*

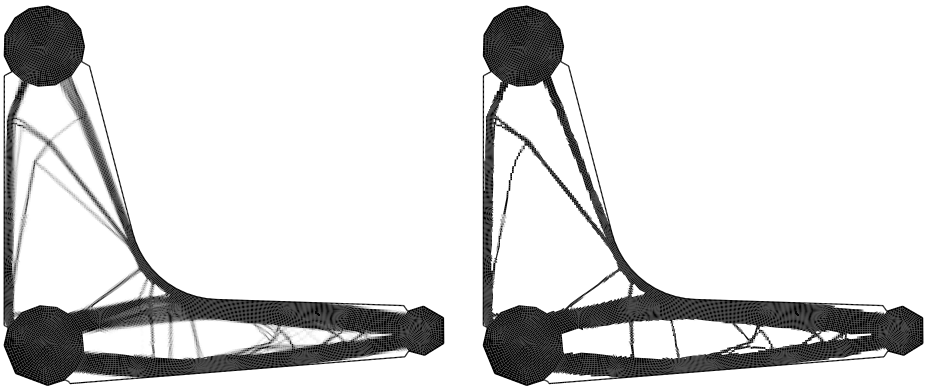

Figure 12: *Composite (left) and penalized (right) solutions of the suspension triangle optimized by the multiple loads method*

References

[1] W. Achtziger, M. Bendsoe, A. Ben-Tal, J. Zowe, *Equivalent displacement based formulations for maximum strength truss topology design,* IMPACT of Computing in Science and Engineering, 4, pp.315-345 (1992).

[2] G. Allaire, *Explicit lamination parameters for three-dimensional shape optimization,* Control and Cybernetics 23, pp.309-326 (1994).

[3] G. Allaire, *Relaxation of structural optimization problems by homogenization,* "Trends in Applications of Mathematics to Mechanics", M.M.Marques and J.F.Rodrigues Eds., Pitman monographs and surveys in pure and applied mathematics 77, pp.237-251, Longman, Harlow (1995).

[4] G. Allaire, E. Bonnetier, G. Francfort, F. Jouve, *Shape optimization by the homogenization method,* to appear in Numerische Mathematik.

[5] G. Allaire, G. Francfort, *A numerical algorithm for topology and shape optimization,* In "Topology design of structures" Nato ASI Series E, M. Bendsoe et al. eds., 239-248, Kluwer, Dordrecht (1993).

[6] G. Allaire, R.V. Kohn, *Optimal bounds on the effective behavior of a mixture of two well-ordered elastic materials,* Quat. Appl. Math. 51, 643-674 (1993).

[7] G. Allaire, R.V. Kohn, *Optimal design for minimum weight and compliance in plane stress using extremal microstructures,* Europ. J. Mech. A/Solids 12, 6, 839-878 (1993).

[8] M. Avellaneda, *Optimal bounds and microgeometries for elastic two-phase composites,* SIAM J. Appl. Math. 47, 6, 1216-1228 (1987).

[9] M. Avellaneda, G. Milton, *Bounds on the effective elasticity tensor of composites based on two point correlations,* in Proceedings of the ASME Energy Technology Conference and Exposition, Houston, 1989, D. Hui et al. eds., ASME Press, New York (1989).

[10] M. Bendsoe, *Methods for optimization of structural topology, shape and material,* Springer Verlag (1995).

[11] M. Bendsoe, A. Diaz, N. Kikuchi, *Topology and generalized layout optimization of structures,* In "Topology Optimization of Structures" Nato ASI Series E, M. Bendsoe et al. eds., pp.159-205, Kluwer, Dordrecht (1993).

[12] M. Bendsoe, N. Kikuchi, *Generating Optimal Topologies in Structural Design Using a Homogenization Method,* Comp. Meth. Appl. Mech. Eng. 71, 197-224 (1988).

[13] F. Brezzi, M. Fortin, *Mixed and hybrid Finite Element Methods,* Springer, Berlin, 1991.

[14] G. Cheng, N. Olhoff, *An investigation concerning optimal design of solid elastic plates,* Int. J. Solids Struct. 16, pp.305-323 (1981).

[15] R. Christensen, *Mechanics of Composite Materials,* Wiley-Interscience, New York (1979).

[16] H. Eschenauer, V. Kobelev, A. Schumacher, *Bubble method of topology and shape optimization of structures,* Struct. Optim. 8, pp.42-51 (1994).

[17] G. Francfort, F. Murat, *Homogenization and Optimal Bounds in Linear Elasticity,* Arch. Rat. Mech. Anal. 94, 307-334 (1986).

[18] G. Francfort, F. Murat, L. Tartar, *Fourth Order Moments of a Non-Negative Measure on S^2 and Application,* to appear in Arch. Rat. Mech. Anal. (1995).

[19] Y. Grabovsky, R. Kohn, *Microstructures minimizing the energy of a two-phase elastic composite in two space dimensions II: the Vigdergauz microstructure,* to appear.

[20] V. Hammer, M. Bendsoe, R, Lipton, P. Pedersen, *Parametrization in laminate design for optimal compliance,* preprint (1996).

[21] Z. Hashin, *The elastic moduli of heterogeneous materials,* J. Appl. Mech. 29, 143-150 (1963).

[22] Z. Hashin, S. Shtrikman, *A variational approach to the theory of the elastic behavior of multiphase materials,* J. Mech. Phys. Solids 11, 127-140 (1963).

[23] C. Jog, R. Haber, M. Bendsoe, *Topology design with optimized, self-adaptative materials,* Int. Journal for Numerical Methods in Engineering 37, 1323-1350 (1994).

[24] U. Kirsch, *Optimal topologies of truss structures,* Comp. Meth. Engrg. 72, pp.15-28 (1989).

[25] R. Kohn, G. Strang, *Optimal Design and Relaxation of Variational Problems I-II-III,* Comm. Pure Appl. Math. 39, 113-182,353-377 (1986).

[26] R. Lipton, *On optimal reinforcement of plates and choice of design parameters,* Control and Cybernetics 23, pp.481-493 (1994).

[27] K. Lurie, A. Cherkaev, A. Fedorov, *Regularization of Optimal Design Problems for Bars and Plates I,II,* J. Optim. Th. Appl. 37, pp.499-521, 523-543 (1982).

[28] A. Michell, *The limits of economy of material in frame-structures,* Phil. Mag. 8, 589-597 (1904).

[29] G. Milton, *On characterizing the set of possible effective tensors of composites: the variationnal method and the translation method,* Comm. Pure Appl. Math. 43, 63-125, (1990).

[30] F. Murat, *Contre-exemples pour divers probèmes où le contrôle intervient dans les coefficients,* Ann. Mat. Pura Appl. 112, 49-68 (1977).

[31] F. Murat, L. Tartar, *Calcul des variations et homogénéisation,* in Les méthodes de l'homogénéisation : théorie et applications en physique, Coll. de la Dir. des Etudes et Recherches EDF, pp.319-370, Eyrolles, Paris (1985).

[32] N. Olhoff, M. Bendsoe, J. Rasmussen, *On CAD-integrated structural topology and design optimization,* Comp. Meth. Appl. Mechs. Engng. 89, pp.259-279 (1992).

[33] O. Pironneau, *Optimal shape design for elliptic systems,* Springer Verlag, Berlin (1984).

[34] W. Prager, G. Rozvany, *Optimal layout of grillages,* J. Struct. Mech. 5, 1-18 (1977).

[35] G. Rozvany, M. Bendsoe, U. Kirsch, *Layout optimization of structures,* Applied Mechanical reviews 48, 2, pp.41-118 (1995).

[36] K. Suzuki, N. Kikuchi, *A homogenization method for shape and topology optimization,* Comp. Meth. Appl. Mech. Eng. 93, 291-318 (1991).

[37] L. Tartar, *Estimations Fines des Coefficients Homogénéisés,* Ennio de Giorgi colloquium, P. Krée ed., Pitman Research Notes in Math. 125, 168-187 (1985).

[38] S. Vigdergauz, *Effective elastic parameters of a plate with a regular system of equal-strength holes,* Mech. Solids 21, 162-166 (1986).

[39] M. Zhou, G. Rozvany, *The COC algorithm, Part II: Topological, geometrical and generalized shape optimization,* Comp. Meth. App. Mech. Engrg. 89, 309-336 (1991).